CHAPTER 1

INTRODUCTION

Precipitation is one of the most difficult of all atmospheric variables to measure, mainly because it has a highly skewed distribution in space and time. Rain-gauge networks are very sparse or even nonavailable over vast deserts, mountains, and jungle areas and over oceans, which makes satellite-derived retrievals the only way to obtain rainfall estimates over the above areas. The accuracy of the satellite remote sensing estimation largely depends on retrieval techniques, which are always based on some assumptions and never perfect. Among all kinds of precipitation systems, tropical cyclones are probably the most important because they occasionally cause major disasters on human being and they may contribute large percent of beneficial rainfall for agriculture in many regions (Rodgers et al. 2000; 2001). They are also probably the most difficult kind to quantitatively estimate precipitation because they usually develop and grow over ocean and during landfall high winds often compromise rain measurements in land.

1.1 Tropical Cyclones

According to the definition given by the National Hurricane Center (NHC), tropical cyclones are warm-core nonfrontal synoptic-scale cyclones. They originate over tropical or subtropical waters, with organized deep convection and a closed surface wind circulation about a well-defined center. When a maximum 10-minute average wind speed in the range of 28 to 33 knots, the storm is called a tropical depression. When the maximum 10-minute average winds reach 34 knots, it becomes a tropical storm, and a tropical cyclone at 64 knots. A tropical cyclone is also called a hurricane if it is over the North Atlantic Ocean or a typhoon if it is over the North Pacific Ocean. The winds that swirl about the center decrease with height, but typically fill the whole troposphere (Haurwitz 1935). The inner core region in a tropical cyclone contains the spiral bands of precipitation, the eyewall, and the eye that differentiates tropical cyclones from any other meteorological phenomena. Willoughby et al. (1982, 1984) proposed that the storm's radar structure can be identified as the stationary band complex (SBC) that consistents of an eyewall, a principal rainband, connecting bands, and several secondary rainbands outside the eyewall. The eyewall region is a quasi-circular ring of convection surrounding the circulation center. Once formed, a tropical cyclone is maintained by the extraction of heat energy from ocean at high temperature and heat export at the low temperatures of the upper troposphere.

Tropical cyclones are an important source of rainfall for agriculture and other water applications over the regions of subtropics and tropics. Climatological studies show that tropical cyclones contribute approximately 7% and 4% of the total rainfall in the entire domain of the North Pacific and North Atlantic, respectively, during tropical cyclone season, with maximum regional contributions of about 30% (Rodgers et al. 2000, 2001).

As a main energy source for the development and maintenance of tropical cyclones, the release of latent heat is directly related to the tropical cyclone intensity (Adler and Rogers 1977; Rodgers and Adler 1981; Rao and MacArthur 1994; Rodgers et al. 1994a,b). The surface rain rate and the vertical distribution of hydrometeor profiles can be used directly to estimate the latent heat release. So the rainfall rate, ice water content (IWC), and liquid water (LWC) have implications for tropical cyclone intensity. High correlations were found between the future tropical cyclone intensity and satellite-based 85-GHz ice-scattering signature within 1° radius of the cyclone center (Cecil and Zipser, 1999) and rainfall rates within the 2° radius of the center of typhoons (Rao and MacArthur, 1994).

However, predicting rainfall and intensity associated with tropical cyclones is a major operational challenge. Although track forecasts continue to improve, quantitative precipitation and intensity forecasts have shown little skill (DeMaria and Kaplan 1999). Accurate quantitative rainfall and hydrometeor content estimation, and therefore latent heating estimation, within tropical cyclones over ocean is a difficult problem because there are no direct measurements available. Research aircraft can fly through the storm and provide precipitation estimates from passive and active instruments. The flight-level microphysics observations represent the limited but important data source to help those estimations. At the same time, the Tropical Rainfall Measuring Mission (TRMM, Simpson et al. 1988, 1996; Kummerow et al. 1998, 2000) satellite provides both radar vertical structure information and high resolution passive microwave observations over Tropics. With the long period of coverage over oceans, one of the TRMM goals is to obtain the four-dimensional structure of latent heating in the tropical atmosphere. TRMM can obtain about 700 overpasses of tropical cyclones each year, which is an important data source for study of this unique system.

1.2 Background of Microwave Remote Sensing

1.2.1 Overview

Microwave remote sensing uses microwave radiation at wavelengths from about 1 mm to about 10 cm (or at frequencies from about 300 GHz to 3 GHz). One of the main attractions of the microwave band is the relative transparency of clouds at these wavelengths, so that some properties of the surface and of the atmospheric column can be estimated under nearly all-weather condition. In contrast, the IR radiation could seriously be interfered with by even thin clouds.

There are two types of microwave remote sensing: passive and active. Passive microwave sensors, often referred to as microwave radiometers, are receivers that measure the radiation emanating from the scene under observation. Active microwave sensors, often referred to as radar, provide their own source of illumination and measure backscattering from cloud and precipitation.

Microwave radiation propagating in the atmosphere is absorbed by atmospheric gases and absorbed and scattered by hydrometeors. Both *absorption* and *scattering* remove energy from a beam of radiation traversing the medium. The beam of radiation is attenuated, and we call this attenuation *extinction*. Thus, extinction is a result of absorption plus scattering. In the field of radiative transfer, it is customary to use a term called *cross section* σ, analogous to the geometrical area of a particle, to denote the amount of energy removed from the original beam by the particle. When the cross section is associated with a particle dimension, it units are denoted in terms of area (m^2). Thus, the extinction cross section σ_e, in units of area, is the sum of the absorption and scattering cross sections ($\sigma_a + \sigma_s$). However, when the cross section is in reference to unit mass, its units are given in area per mass (m^2/kg) and we call it *mass extinction cross* *section* (k_e). But usually we call k_e *mass extinction coefficient* ($k_e = k_a + k_s$, where k_a and k_s are *mass absorption coefficient* and *mass scattering coefficient*). Furthermore, when the extinction cross section σ_e is multiplied by the particle number density N (m^{-3}), or when the mass extinction coefficient is multiplied by the density (kg/m^3), the quantity is referred to as the *extinction coefficient* (β_e), whose units are given in terms of length (m^{-1}), then we have

$$\beta_e = \int N(D)\sigma_e(D)dD \tag{1.1}$$

where *D* is the equivalent spherical particle diameter and *N(D)* is the particle number concentration in diameter interval from *D* to *D+dD*.

Emission is the process by which some of the internal energy of a material is converted into radiant energy. Emission by a blackbody is the converse of absorption. The intensity of radiation emitted by a blackbody with a physical temperature *T* is given by Planck's Function $B(T)$:

$$B_\lambda(T) = \frac{2hc^2}{\lambda^5(e^{hc/k_B\lambda T} - 1)} \tag{1.2}$$

where λ is wavelength, $c = 3\times10^8$ m/s is the speed of light, $h = 6.626\times10^{-34}$ J is Planck's constant, and $k_B = 1.381\times10^{-23}$ J/K is Boltzmann's constant. In microwave remote sensing of the atmosphere, the wavelengths of interest are quite long -- $\lambda \sim 1$ mm or longer. In the limit of large wavelength,

$$B_\lambda(T) \approx \frac{2ck_B}{\lambda^4}T \tag{1.3}$$

in which case blackbody emission is seen to be proportional to absolute temperature. This so-called Rayleigh-Jeans approximation significantly simplifies some kinds of radiative transfer calculations in the microwave band. Blackbody is the idealization of any real object, and the Planck's function is the theoretical maximum possible emission from any real object. *Emissivity* ε_λ is defined as the ration of what is emitted by an object to what would be emitted if it were a blackbody. *Absorptivity* a_λ is defined as the ration of what is absorbed by an object to what would be absorbed if it were a blackbody. The relationship between absorptivity and emissivity is embodied succinctly by Kirchhoff's Law, which states that

$$\varepsilon_\lambda = a_\lambda \tag{1.4}$$

The microwave emissivities of natural surface are often considerably less than unity and may in fact vary wildly from one scene to the next. In particular, the land surface emissivities are typically as large as 0.8-0.95, whereas ocean surface emissivities may be as small as 0.25-0.7. This variation in surface emissivity makes it much more difficult to use microwave imagery for accurately estimating surface temperature, but greatly facilitates the determination of other surface properties.

The microwave radiometer measures the radiance, which is usually converted into the equivalent blackbody temperature or *brightness temperature* T_b by using the Planck's Function. A particularly convenient property of the microwave band is the validity of the Rayleigh-Jeans approximation, which allows us to work with brightness temperature as a convenient stand-in for radiant intensity. Because of the proportionality between blackbody radiance and temperature in the microwave band, there is a very simple relationship between T, ε_λ, and T_b:

$$T_b \approx \varepsilon_\lambda T \tag{1.5}$$

1.2.2 Passive Microwave Remote Sensing of Precipitation

Passive microwave radiometers have been carried on satellites for climatic-scale precipitation observations since 1972 (Arkin and Ardanuy, 1989). They measures radiances that are the integrated effect of absorption/emission and scattering through a precipitating cloud along the sensor path view. Consider the passage of radiation of wavelength λ through a layer of atmospheric medium with infinitesimal thickness ds, measured along the direction of propagation. If the radiant intensity is initially I, the change of I (dI) along ds can be written as:

$$dI = dI_{ext} + dI_{emit} + dI_{scat}$$

(1.6)

where the depletion due to extinction (both absorption and scattering) is given by

$$dI_{ext} = -\beta_e I ds \tag{1.7}$$

where the extinction coefficient is the sum of the absorption coefficient and scattering coefficient, i.e., $\beta_e = \beta_a + \beta_s$. The source due to emission is

$$dI_{emit} = \beta_a B(T) ds \tag{1.8}$$

where $B(T)$ is the Planck's function. The source due to the radiation from any direction θ' scattered into the beam in the direction of interest θ is

$$dI_{scat} = \frac{\beta_s}{4\pi}\int_{4\pi} p(\theta',\theta)I(\theta')d\omega' ds \tag{1.9}$$

where the scattering phase function $p(\theta',\theta)$ is required to satisfy the normalization condition

$$\frac{1}{4\pi}\int_{4\pi} p(\theta',\theta)d\omega' = 1 \tag{1.10}$$

The complete differential form of the radiative transfer equation can be written as

$$dI = -\beta_e I ds + \beta_a B ds + \frac{\beta_s}{4\pi}\int_{4\pi} p(\theta',\theta)I(\theta')d\omega' ds \tag{1.11}$$

This is the most general and complete form of the radiative transfer equation. In the microwave band, because of the Rayleigh-Jeans approximation the radiant intensity I and the Planck's function B in (1.11) can be substituted by T_b and T.

The calculation of (1.11) is very complex due to the existence of the scattering source term (the last term of (1.11) on the right hand side), which requires a solution for the intensity field not just in one direction along a one-dimensional path but for all directions simultaneously in three-dimensional space. One would therefore like to be able to neglect scattering (as a source, at least) whenever possible. So the question is, "when does scattering matter?" The scattering component of the radiative transfer equation (1.11) depends on the local scattering coefficient and the scattering phase function. These in turn depend both on wavelength and on the size, phase, and number of particles. The size of a particle is the most important defining characteristic. In general, particles that are far smaller than the wavelength will scatter only very weakly.

A nondimensional *size parameter* x is defined as:

$$x \equiv \frac{2\pi r}{\lambda} \tag{1.12}$$

where r is the radius of a spherical particle. Given the value of x, one can immediately determine whether scattering by the particle is likely to be significant and, if so, which broad scattering regime – Rayleigh, Mie, or geometric optics – is most applicable. Fig. 1.1 represents how various combinations of particle type and wavelength relate to these regimes. From Fig. 1.1, we see that in the microwave band (1 mm < λ < 10 cm), the size parameters of all atmospheric particles from small air molecules to large hails are in negligible scattering, Rayleigh, or Mie regimes (Petty 2004).

In the field of the quantitative precipitation estimation using passive microwave remote sensing, basically there are two types of algorithms based on if the scattering effect can be neglected or not: *emission-based* and *scattering-based* (the profiling algorithm as mentioned later is just the combination of these two).

Emission-based algorithms are based on the downward-looking microwave radiometer observations on low frequencies. For frequency less than 19 GHz (wavelength greater than 1.55 cm), almost all precipitation particles except large hails, which are beyond the consideration of this study on tropical oceanic rainfall systems, are in Rayleigh scattering regime according to Fig. 1.1. The Mie theory gives the extinction (absorption and scattering) cross section for a sphere as a function of size parameter x and relative index of refraction m as follow:

$$\sigma_e = \frac{\lambda^2}{2\pi} \mathrm{Re} \sum_{n=1}^{\infty} (2n+1)(a_n + b_n) \tag{1.13}$$

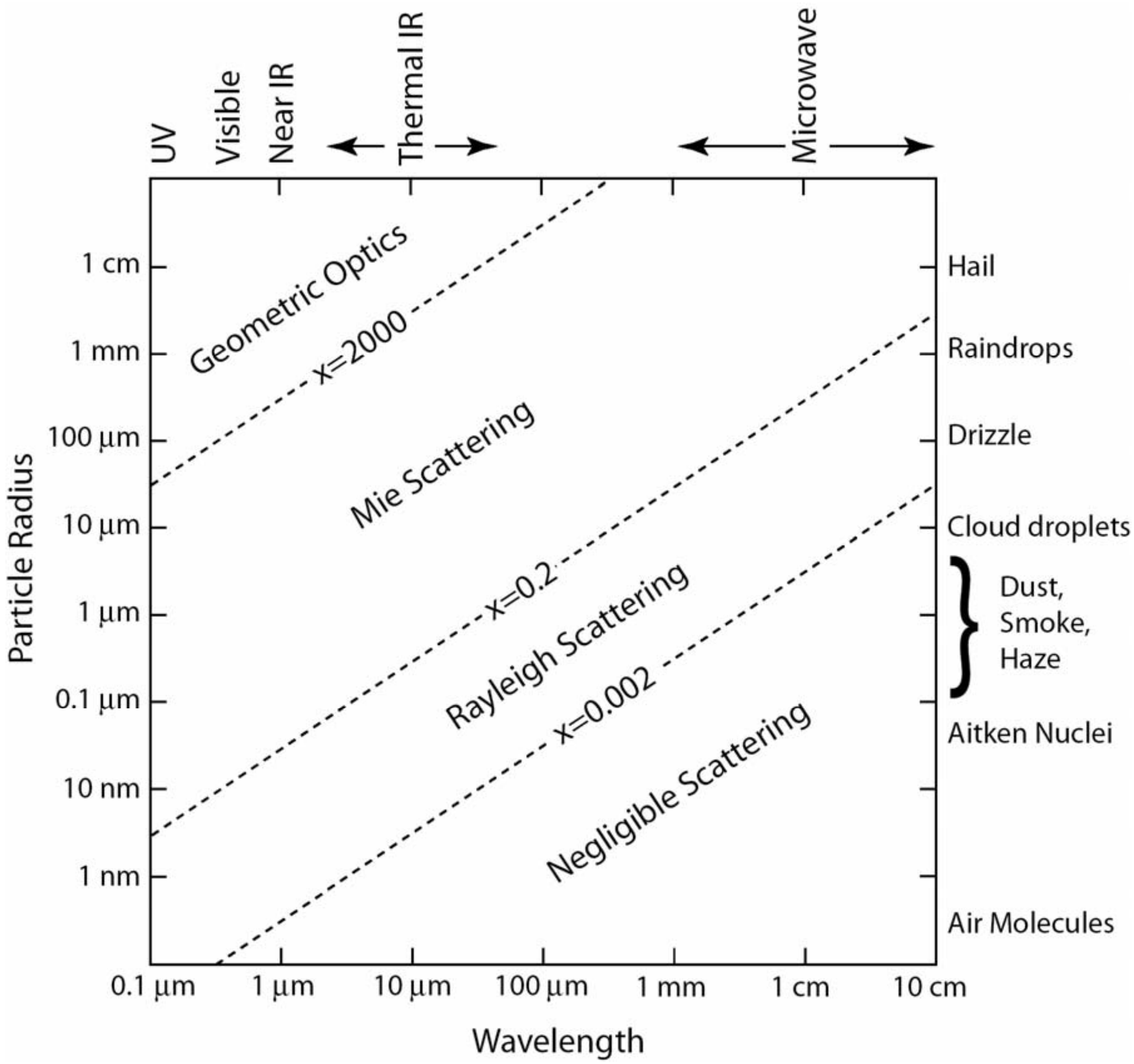

Figure 1.1. Relationship between particle size, radiation wavelength and scattering behavior for atmospheric particles. Diagonal dashed lines represent rough boundaries between scattering regimes (reprinted with permission from Petty 2004).

$$\sigma_s = \frac{\lambda^2}{2\pi}\sum_{n=1}^{\infty}(2n+1)(|a_n|^2 + |b_n|^2) \tag{1.14}$$

where the coefficients a_n and b_n are referred to as Mie scattering coefficients and are functions of *x* and *m*. (1.13) and (1.14) are valid for both Rayleigh and Mie scattering regime. In particular, for Rayleigh regime (*x* is small enough), the scattering and absorption cross section simplifies to:

$$\sigma_s = \frac{16\pi r^2}{3} x^4 \left|\frac{m^2 - 1}{m^2 + 2}\right|^2 \tag{1.15}$$

$$\sigma_a = 4\pi r^2 x \,\mathrm{Im}\{\frac{m^2 - 1}{m^2 + 2}\} \tag{1.16}$$

We see that the absorption cross section is proportional to r^3, while the scattering cross section is proportional to r^6. So for sufficiently small liquid particles (for liquid, *m* has a nonzero imaginary part), the scattering is insignificant. Thus, $\sigma_e \approx \sigma_a$, and the mass extinction coefficient k_e can be expressed as:

$$k_e = \frac{\sigma_a}{\rho(4/3)\pi r^3} = \frac{6\pi}{\rho\lambda}\mathrm{Im}\{\frac{m^2 - 1}{m^2 + 2}\} \tag{1.17}$$

where ρ is the density of the particle. Note that there is no dependence of k_e on the particle radius *r*. Therefore, for radiation passing through a cloud of sufficiently small absorbing particles, the total absorption is proportional to the total mass path, regardless of the exact sizes of the constituent particles. At low frequencies, this condition is quite valid for particles radius less than 100 μm in nonrainning clouds.

The Mie theory-based calculations by Wilheit et al. (1997) presented both extinction and absorption coefficients for raindrops at 19 GHz for a Marshall-Palmer distribution of raindrops as a function of rain rate (see Fig. 1 of Wilheit et al. 1997). Their results show how the extinction is defined by the rain rate and furthermore how the extinction at this frequency is largely governed by absorption processes since the scattering coefficient is almost an order of magnitude smaller than the absorption coefficient. Another important finding by Wilheit et al. (1977) is that the rain rate and absorption coefficients represents similar moments (although they are not three moments as in Rayleigh approximation) of the raindrop size distribution. Thus, although both the brightness temperature and rain rate are individually dependent on the drop size distribution, the relationship between the two should not be excessively dependent on the details of the particle size distribution (see their Fig. 5).

After neglecting scattering, it is straightforward in principle to derive the brightness temperature associated with upwelling radiation as a function of rain rate based on (1.11). Emission from raindrops, when viewed against a cold ocean background, increases with increasing optical depth. This increased emission, measured as an increased brightness temperature, is then associated with the rain rate. Fig. 1.2 shows an example of the relationship from the radiative transfer simulation. The calculated brightness temperature at 10.7 GHz is presented as a function of the modeled rain rate. From Fig. 1.2, we see that the 10.7 GHz brightness temperature increases with rain rate increasing up to 50 mm/hr without saturation. For less than 10 GHz microwave channels, the saturation limit of rain rate will be even larger. As will be mentioned in Chapter 2, the Stepped Frequency Microwave Radiometer (SFMR) on the NOAA P3 aircraft has six frequencies

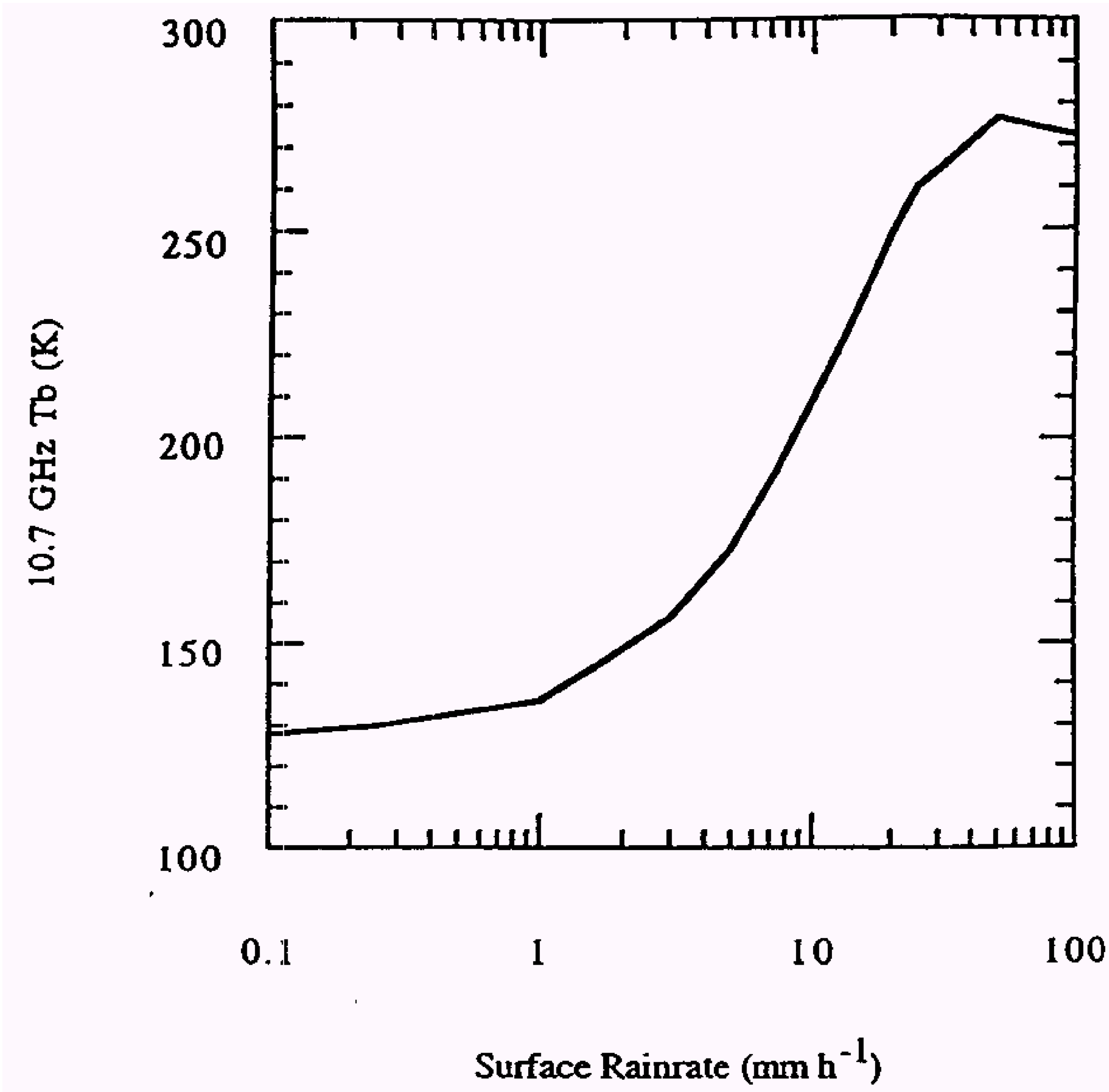

Figure 1.2. Relationship between nadir 10.7-GHz brightness temperature and surface rain rate over the tropical ocean using the model described by Kummerow and Weinman 1998 (reprinted with permission from McGaughey et al. 1996).

between 4.55 to 7.22 GHz. It has the ability to estimate very heavy rain rate using the emission-based algorithm. For TRMM, emission-based algorithms usually use 10 GHz channel to estimate large rain rates and use 19 GHz channel to estimate smaller rain rates since 19 GHz is more sensitive to small rain rate values but saturates for rain rate larger that 15-20 mm/hr.

Fig. 1.3 shows the brightness temperature - rain rate relationships at 18, 37, and 85.6 GHz from the radiative transfer modeling for over land and over ocean. From Fig. 1.3, the brightness temperature - rain rate relationship over ocean for 18 GHz is complex. For rain rate less than 15 mm/hr, Tb increases as rain rate increases. But for rain rate larger than 15-20 mm/hr, scattering by the large ice crystals over regions of heavy rainfall confuses matters. Radiation emitted from the underlying rain is scattered downward by the overlying layer of ice particles and away from any instrument looking downward above the cloud. This increase in scattering as rain rate increases (or exactly ice water path increases) leads to a decrease in brightness temperature. This is what the *scattering-based* algorithm is based on.

Scattering-based algorithms use microwave observations at high frequencies (greater than 37 GHz). For these channels, the size parameters for cloud and precipitation particles are usually between 1~6, so it is in Mie scattering regime. The scattering effect of frozen hydrometeors for these channels is not negligible. Thus, the complete radiative transfer equation (1.11) needs to be solved including emission, absorption, and scattering effects of liquid, combined phase, and ice hydrometeors. The first of this kind of microwave radiative transfer model is presented by Wu and Weinman (1984) and Kummerow and Weinman (1988). Their simulation results show that the presence of ice hydrometeors markedly depresses the brightness temperatures at 37 and 86 GHz, which

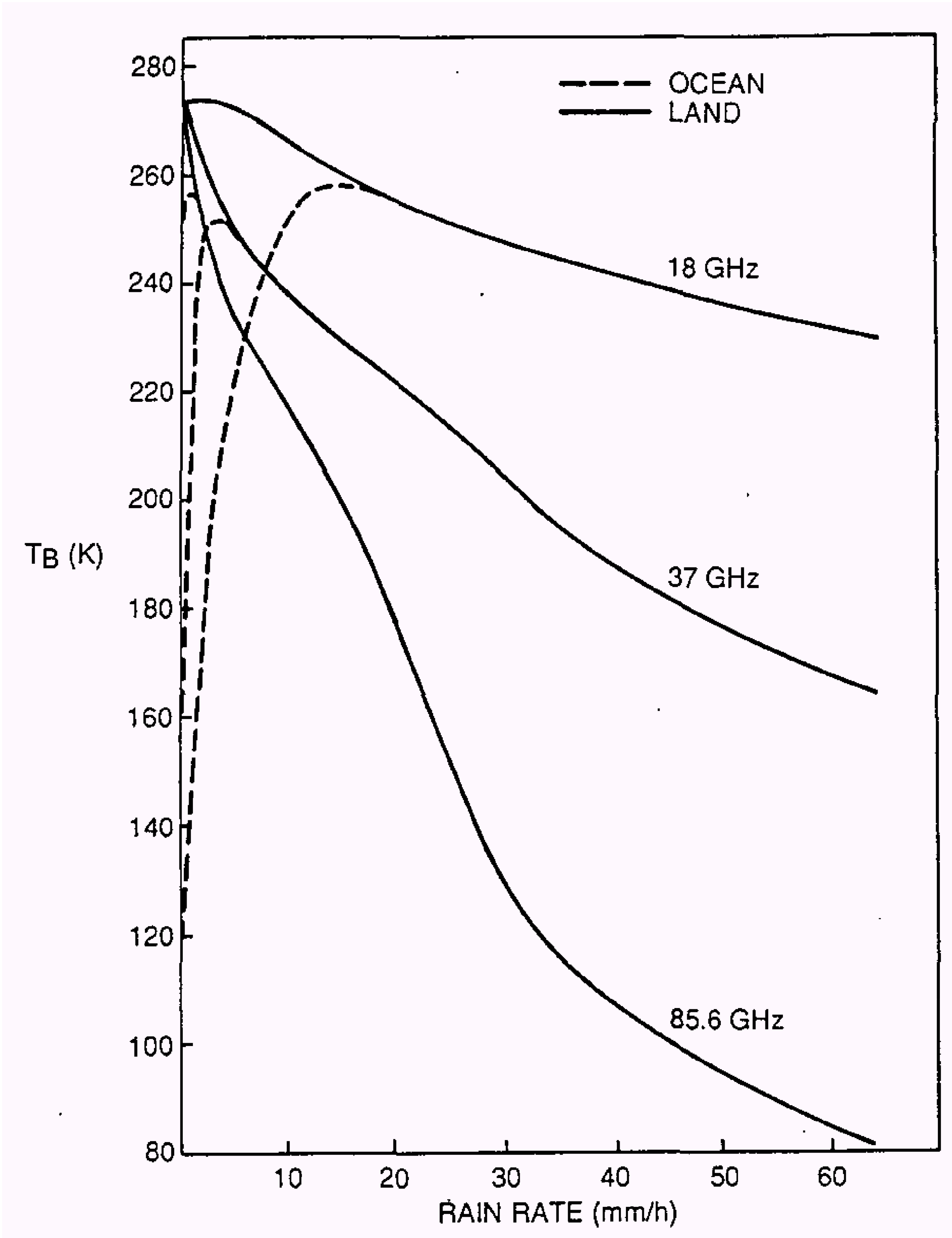

Fig. 1.3. Brightness temperature - rain rate relationships at 18, 37, and 85.6 GHz from the radiative transfer modeling of Wu and Weinman (1984). The vertical distribution of hydrometeors was based upon averaged radar results and assumed ice precipitation above and liquid precipitation below the freezing level (reprinted with permission from Spencer et al. 1989).

is consistent with satellite microwave radiometer observations. Fig. 1.3 also shows the depression of the calculated brightness temperature at 37 and 85.6 GHz as a function of the modeled rain rate. In the simulation of Fig. 1.3, the amount of frozen hydrometeors increases with increasing the rain rate. In fact, the direct relationship is between the total ice water path (instead of rain rate) and the brightness temperature depression.

Unlike emission based retrievals, which are not excessively sensitive to particle size distribution, scattering based retrievals are very sensitive to particle size distribution the particle size distribution (PSD. In the following text, the PSD will be used to represent both rain drop size distribution and ice particle size distribution). Fig. 1.4 depicts the Mie scattering extinction efficiency Q_e ($Q_e = \sigma_e / \pi r^2$) calculated from (1.13) as a function of size parameter x for a sphere with $m = 1.78$. This is representative value for ice in the microwave band. Note that no imaginary part is assumed in m, so the ice particle is nonabsorbing, which means $Q_a = 0$ and $Q_e = Q_s$. The real value of the imaginary part of m for ice at frequencies from 37 ~ 85 GHz varies from 0.007 to 0.0054 as temperature varies from 0 to $-70^\circ C$. But these small values do not bring much absorption therefore do not change the Q_e curve very much. From Fig. 1.4a, we see that the relationship between extinction (scattering only here) efficiency Q_e and size parameter is very complex. Q_e starts at 0 for $x = 0$ and rises monotonically up to about $x = 2.5$ (for 85 GHz, it represents ice particles with size less than 3 mm; for 37 GHz, it represents ice particles with size less than 6 mm), where Q_e achieves a maximum value of about 5. In other words, for this value of x, the ice particle scatters five times as much radiation as one might surmise from its cross sectional area alone. Thereafter, it exhibits an even-dampening oscillation about a mean value of 2, which is the limiting value of Q_e for large x. At the other end of the range, we compare Q_e (=Q_s) computed using the exact Mie

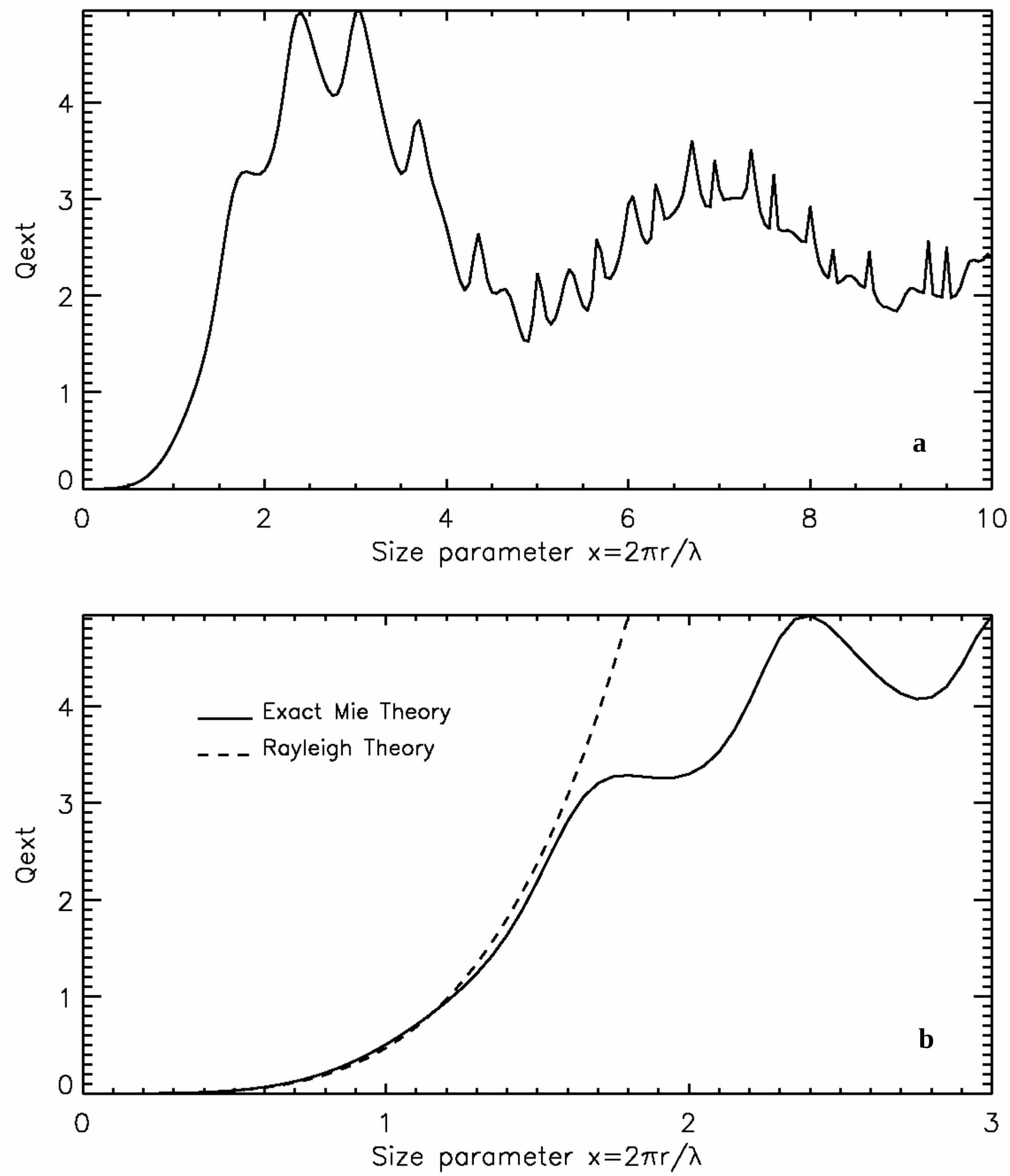

Figure 1.4. The extinction efficiency Q_e as a function of size parameter x for a nonabsorbing ice sphere with m=1.78, for various of x. (a) Detail for x < 10; (b) Detail for x < 3, comparing the Rayleigh (small particle) approximation and exact Mie theory.

theory with that obtained for the small-particle (Rayleigh) limit (Fig. 1.4b). We can see that the agreement is quite good up to about $x = 1.2$. Beyond that point, Q_e increases less rapidly than the x^4 dependence predicted by (1.15). So for $x < 1.2$, the extinction coefficient β_e in (1.1) is proportional to D^6 as in Rayleigh regime. For $1.2 < x < 6$, the relation between β_e and particle diameter D is not monotonically according to Fig. 1.4a.

The bulk parameters of precipitation that we most concern are rain rate (R) and water content (M) defined as:

$$R = \int_0^\infty N(D)V(D)D^3 dD \tag{1.18}$$

$$M = \frac{\pi}{6}\int_0^\infty N(D)\rho D^3 dD \tag{1.19}$$

where ρ is the density of liquid or ice particles, and V(D) is the terminal fall velocity of raindrops, which is approximately proportional to $D^{0.5}$ to D^1 for raindrops and frozen hydrometeors depending on their sizes and habits, etc. (Rodgers and Yau 1989; Pruppacher and Klett, 1997). From (1.18) and (1.19), R is proportional to $V(D)D^3$ and M is proportional to D^3. Therefore we can not estimate R and M from β_e without knowing a specific PSD.

1.2.3 Active Microwave Remote Sensing of Precipitation

As one of active microwave remote sensing instruments, radar has become one of the most important observational tools of operational meteorologists. Weather radar, in wavelengths of 2-10 cm, allows the monitoring of rainfall with far more detail in both time and space than is possible with conventional rain gauges. Radar measures the backsattering of cloud and precipitation particles. Following the definition of the extinction cross section in section 2.1, the backscattering or radar cross section σ_b is related to the fraction of incident wave power scattering backward (180° scattering angle). The Mie equation yielding the solution for σ_b is:

$$\sigma_b = \frac{\lambda^2}{2\pi}\left|\sum_{n=1}^{\infty}(-1)^n(2n+1)(a_n - b_n)\right|^2 \tag{1.20}$$

where the coefficients a_n and b_n are as same as those in (1.13) and (1.14). For most weather radars, almost all precipitation hydrometeors can be considered small compared to the wavelength, so the Rayleigh approximation applies and in Rayleigh regime σ_b becomes:

$$\sigma_b = \frac{\pi^5 D^6}{\lambda^4}\left|\frac{m^2-1}{m^2+2}\right|^2 \tag{1.21}$$

The radar reflectivity η (similar as extinction coefficient β_e in (1.1)) is defined as the sum of the single particle backscattering coefficients per unit volume. η is expressed by:

$$\eta = \int_0^{\infty} N(D)\sigma_b(D)dD \tag{1.22}$$

For Rayleigh scattering, η can be replaced by the radar reflectivity factor, Z, defined by:

$$Z = \frac{\lambda^4 \eta}{\pi^5\left|\frac{m^2-1}{m^2+2}\right|^2} = \int_0^{\infty} N(D)D^6 dD \tag{1.23}$$

The standard radar system determines the water equivalent radar reflectivity factor (*Ze*) by assuming that the complex index of refraction *m* is as same as that for water. So for ice particles, the radar reflectivity factor *Zi* is usually 7 dB higher than radar measured *Ze* because the difference of the complex index of refraction between water and ice (Rinehart 1997). For simplicity, we use *Z* as equivalent radar reflectivity factor instead of *Ze* in the folowing text, and we will call both *Z* and *dBZ=10log10(Z)* as the radar reflectivity.

The advantage of a spaceborne downlooking radar is to provide vertical profiles of radar reflectivities, which are related to the vertical distribution of rain rate and water content, thereafter latent heat release. From (3.1), however, we see that radar reflectivity is proportional to D^6. However, from (1.18) and (1.19), rain rate R is proportional to $V(D)D^3$ and water content M is proportional to D^3, so the inversion from Z to R or M is impossible without knowing *N(D)*, the PSD. The Z-R relationship can be expressed by

$$Z = aR^b \tag{1.24}$$

where *a* and *b* are constant for a specific PSD. The Z-M relationship is similar as (1.24).

Unfortunately, PSD has a large varibility for different environment conditions and precipitation types. Studies have show that the rain PSD fluctuations limit the rain rate measurement accuracy to ~30-40% on average, if a single climatological Z-R relationship is used (Chandrasekar et al. 2003). This accuracy could be improved significantly if the Z-R relationship is adjusted based on precipitation type.

1.2.4 Beamfilling Problem of Space-based Microwave Observations

The space-based radiometer and radar observations may provide accurate precipitation measurements with nearly global coverage. However, one difficulty in retrieving rain rate and hydrometeor content from space-based platform is correcting for the so-called beamfilling effect. For spaced-based microwave instruments, the foot print size or field of view (FOV) is usually larger than the typical size of rain cells. This implies that the rainfall within the FOV may not be uniformly spread, especially when observing convective rainfall. The beamfilling problem comes about because the radiometer or radar measures a FOV area average microwave brightness temperature T_b or radar reflectivity factor Z, while the observer desires an estimate of the FOV area average rain rate R or water content M. The problem is that the formula relating the point value of T_b or Z and the point value of R or M is nonlinear, which can be see from Fig. 1.2 and (1.24). Hence, straightforward insertion of the measured FOV T_b or Z into the formula does not lead to the FOV average R or M because of the heterogeneity of rainfall within the FOV.

The magnitude of beamfilling error for a specific instrument is dependent on its footprint size. Aircraft radar with a footprint size less than 1 km will almost have no beamfilling problem because the typical convective cell is larger than 1-2 km. An aircraft radiometer would have less beamfilling error than a satellite radiometer because the footprint size of an aircraft radiometer is typically much smaller than that of a satellite radiometer. Radiometers at low frequencies would have more severe beamfilling problem than radiometers at high frequencies because of the much larger footprint size of low-frequency radiometers.

1.3 Inversion Problem and PSD Issues

From section 1.2, we see that the a specific PSD assumption is needed for both radar-only and radiometer-only precipitation retrievals, although the emission based radiometer-only algorithm is not very sensitive to PSD (Wilheit et al. 1977).

In the quantitative precipitation estimation from remote sensing observations, the variability of PSD represents one of the main difficulties surrounding the retrieval of precipitation rates and hydrometeor contents. Observations indicate a significant variability of PSD (Bringi et al. 2003; Heymsfield et al 2002b) in different rain types, synoptic conditions, and geo-locations, implying highly variable Z-R, K-Z, Z-IWC, and Z-IWC relations (K is the attenuation/extinction coefficient β_e for radars). The variation of Z-R, K-R, Z-LWC, and Z-IWC relations in different rain types has been studied extensively for many kinds of precipitation systems including hurricanes. Stout and Mueller (1968) summarized that in radar rainfall estimates there are differences on the order of 150% that can be attributed to different types of rain or different synoptic conditions. Atlas et al. (1999) confirmed the systematic variation of Z-R relations between a sequence of rain types in rainfall systems over the tropical oceans. Delrieu et al. (2000) presented the K-R relation variations among “widespread,” “thunderstorm,” and the intensive long-lasting autumn rain events in Cevennes in France. However, in hurricanes, Jorgensen and Willis (1982) and Willis and Jorgensen (1981) showed no obvious variation of Z-R and Z-LWC between stratiform and convective rain types, while Black (1990) gave very different Z-IWC relations for different rain types. Houze et al. (1992) referred to the hurricane as a giant “mixmaster” that stirs and tends to homogenize the precipitation region lying just outside the eyewall. Questions arising here are, “*In the special hurricane precipitation environment, could we expect a near-independence of*

PSD in the rain region for different rain types? How does the PSD issue affect on the microwave precipitation retrieval? Could PSD parameters be retrieved along with hydrometeor profiles by combining radar and radiometer observations?" It is very important to understand the special PSD characteristics in hurricanes, not only for remote sensing retrievals, but also for microphysics parameterization in numerical models, and improving our knowledge of cloud and precipitation processes.

1.4 Outline

In this vein, this research comprises two main objectives, which will address both emission-based passive microwave precipitation retrieval and combined radar-radiometer retrieval algorithms, and also address the PSD variations as a function of rain types in tropical cyclones. In Chapter 2, an emission-based rain rate algorithm in hurricanes from the Stepped Frequency Microwave Radiometer (SFMR) on the National Oceanic and Atmospheric Administration (NOAA) WP-3D aircraft is validated by using simultaneous observations from two radars on the same aircraft. The DSD variability in convective and stratiform regions are investigated. Chapter 3 will formulate a new combined radar-radiometer algorithm to estimate PSD parameters and hydrometeor profiles in tropical cyclones, analyze the error sources by doing sensitivity tests, implement and apply this algorithm to aircraft data, validate it by using independent aircraft *in situ* microphysics and radiometer measurements, compare the retrievals with radar-only and radiometer-only algorithms, and finally apply the combined algorithm to a TRMM hurricane case.